Exocytosis of acid sphingomyelinase by wounded cells promotes endocytosis and plasma membrane repair

Christina Tam,[1,2] Vincent Idone,[1] Cecilia Devlin,[3] Maria Cecilia Fernandes,[2] Andrew Flannery,[2] Xingxuan He,[4] Edward Schuchman,[4] Ira Tabas,[5,6,7] and Norma W. Andrews[1,2]

[1]Section of Microbial Pathogenesis, Yale University School of Medicine, New Haven, CT 06536
[2]Department of Cell Biology and Molecular Genetics, University of Maryland, College Park, MD 20742
[3]Indiana University–Purdue University School of Medicine, Indianapolis, IN 46202
[4]Department of Genetics and Genomic Sciences, Mount Sinai School of Medicine, New York, NY 10029
[5]Department of Medicine, [6]Department of Pathology and Cell Biology, and [7]Department of Physiology and Cellular Biophysics, Columbia University, New York, NY 10027

Rapid plasma membrane resealing is essential for cellular survival. Earlier studies showed that plasma membrane repair requires Ca^{2+}-dependent exocytosis of lysosomes and a rapid form of endocytosis that removes membrane lesions. However, the functional relationship between lysosomal exocytosis and the rapid endocytosis that follows membrane injury is unknown. In this study, we show that the lysosomal enzyme acid sphingomyelinase (ASM) is released extracellularly when cells are wounded in the presence of Ca^{2+}. ASM-deficient cells, including human cells from Niemann-Pick type A (NPA) patients, undergo lysosomal exocytosis after wounding but are defective in injury-dependent endocytosis and plasma membrane repair. Exogenously added recombinant human ASM restores endocytosis and resealing in ASM-depleted cells, suggesting that conversion of plasma membrane sphingomyelin to ceramide by this lysosomal enzyme promotes lesion internalization. These findings reveal a molecular mechanism for restoration of plasma membrane integrity through exocytosis of lysosomes and identify defective plasma membrane repair as a possible component of the severe pathology observed in NPA patients.

Introduction

Early studies performed in sea urchin eggs showed that wounded eukaryotic cells rapidly repair their plasma membrane by a process dependent on extracellular Ca^{2+} (Heilbrunn, 1956; Chambers and Chambers, 1961). However, insights into the cellular mechanism underlying this process were only obtained several decades later, when a functional link was established between plasma membrane repair and the delivery of intracellular membrane to the cell surface by exocytosis (Bi et al., 1995; Miyake and McNeil, 1995). This Ca^{2+}-dependent, exocytosis-mediated resealing process occurs <30 s after plasma membrane injury (Steinhardt et al., 1994) and involves the fusion of lysosomal organelles with the plasma membrane (Rodríguez et al., 1997; Reddy et al., 2001; Jaiswal et al., 2002). Based on these initial findings, two models were proposed for exocytosis-mediated

plasma membrane repair. The first model postulated that Ca^{2+} influx triggers homotypic fusion of intracellular vesicles, forming a patch that directly fuses with the wounded membrane site (McNeil et al., 2000). The second model proposed that resealing of the lipid bilayer is facilitated by reduction in plasma membrane tension, a consequence of Ca^{2+}-triggered exocytosis (Togo et al., 1999).

However, these two models fail to explain the observation that stable lesions caused by pore-forming toxins are also removed from the plasma membrane in a Ca^{2+}-dependent manner (Walev et al., 2001). A recent investigation of this issue revealed that Ca^{2+} influx into wounded cells triggers not only lysosomal exocytosis but also a novel form of endocytosis (Idone et al., 2008b). This unusual form of endocytosis, which occurs within

Correspondence to Norma W. Andrews: andrewsn@umd.edu

Abbreviations used in this paper: ASM, acid sphingomyelinase; BEL, bromoenol lactone; DPA, desipramine; NRK, normal rat kidney; PI, propidium iodide; rhASM, recombinant human ASM; SLO, streptolysin O.

Figure 1. **Inhibition of lysosomal exocytosis in injured cells results in defective endocytosis and plasma membrane repair.** (A) β-Hexosaminidase (βHex) secretion from nontreated (NT) or BEL-treated NRK cells after SLO exposure with or without Ca^{2+}. Error bars represent SD. (B) Nontreated or BEL-treated cells processed for EM 4 min after exposure to SLO/Ca^{2+} and BSA-gold. Short arrows point to BSA-gold particles within endosomes in nontreated cells (NT); long arrows point to swollen ER compartments in BEL-treated cells (BEL). M, mitochondria. (right) EM quantification. The data represent the mean ± SD (**, P < 0.0001; unpaired Student's t test). (C) FACS quantification of WGA-FITC endocytosis after exposure to SLO/Ca^{2+} in nontreated or BEL-treated cells. (D) FACS quantification of PI staining in nontreated or BEL-treated cells permeabilized with SLO. Without Ca^{2+} (middle), both groups of cells remained permeabilized; with Ca^{2+}, nontreated cells resealed their membrane more efficiently, excluding PI (right). (E) FACS quantification of PI staining in nontreated or BEL-treated cells after scrape wounding. Cells treated or not with BEL were similarly wounded, as indicated by the uptake of PI added during scraping (left). PI added 4 min after scraping revealed that both groups remained permeabilized without Ca^{2+} (middle), but with Ca^{2+}, nontreated cells resealed their membrane more efficiently, excluding PI (right). Percentages correspond to resealed (PI negative) cells in the gated region (dashed lines). The results shown in this figure are representative of several independent experiments. Bars, 250 nm.
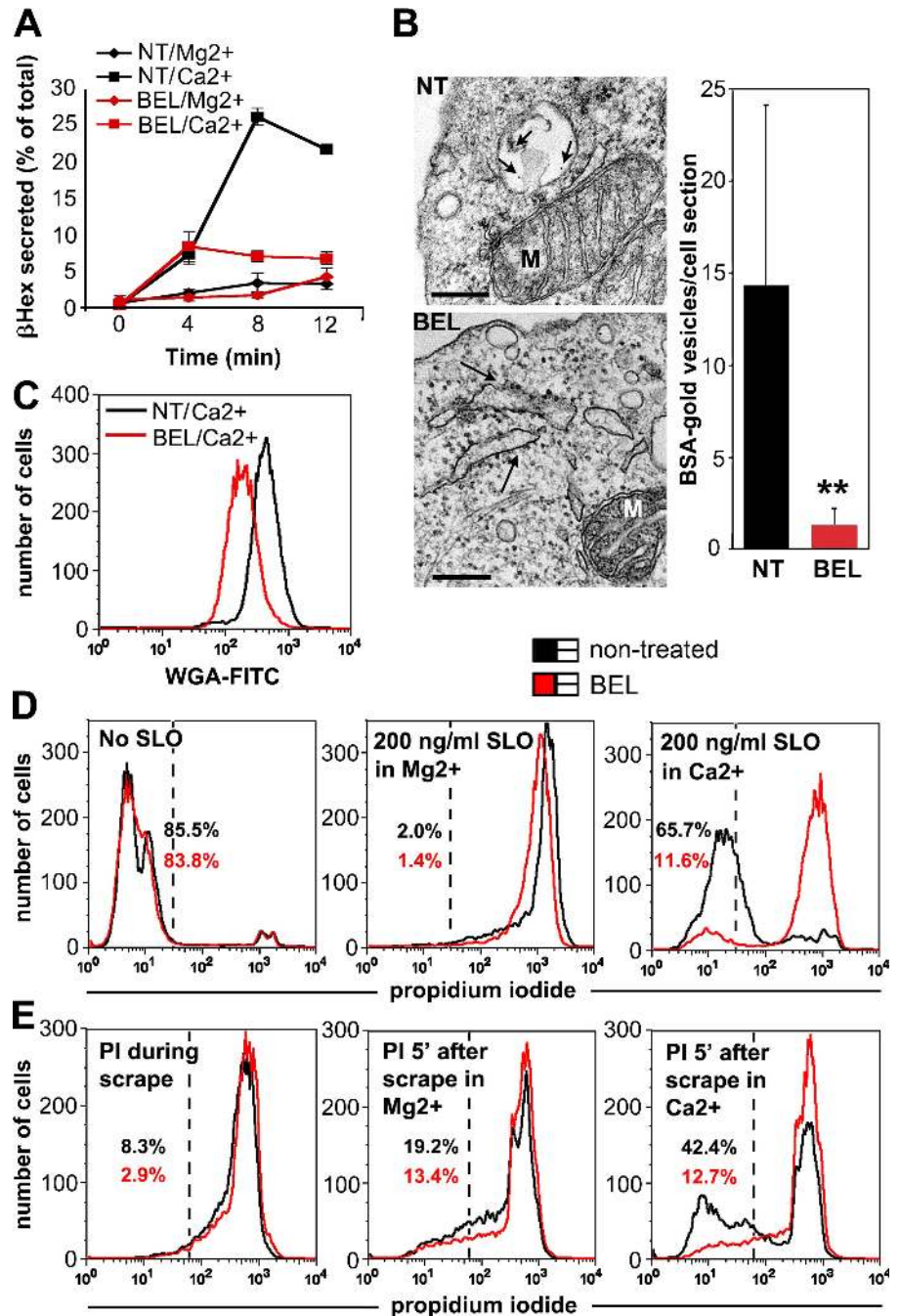
seconds of plasma membrane injury, is dynamin independent, facilitated by disruption of the cortical actin cytoskeleton, and capable of internalizing transmembrane pores. Interestingly, this Ca^{2+}-dependent form of endocytosis is also observed in mechanically injured cells. This finding, together with the very similar kinetics of plasma membrane resealing observed in cells injured mechanically or by pore-forming toxins, led to the proposal of a new general model for plasma membrane repair (Idone et al., 2008a,b). This model postulates that the exocytosis of lysosomes triggered by Ca^{2+} entry through membrane wounds is immediately followed by endocytosis, which mediates lesion internalization and restoration of plasma membrane integrity.

Examination of the morphology of injury-induced endosomes (Idone et al., 2008b) provided an unexpected insight into the molecular mechanism responsible for this novel form of endocytosis. The large, uncoated peripheral endosomes observed in wounded cells strongly resembled the vesicles formed in J774 macrophages after exposure to bacterial sphingomyelinase (Zha et al., 1998). In that study, it was suggested that sphingomyelinase-mediated changes in lipid composition might have created bilayer asymmetries favoring membrane bending and endosome formation (Zha et al., 1998). Subsequent studies confirmed that ceramide, a sphingolipid generated by hydrolytic removal of the phosphorylcholine head group of sphingomyelin by sphingomyelinase, coalesces in membranes to form large domains that are capable of inward budding (Holopainen et al., 2000; Gulbins and Kolesnick, 2003; van Blitterswijk et al., 2003; Grassmé et al., 2007). These findings prompted us to

investigate whether the ceramide-generating lysosomal enzyme acid sphingomyelinase (ASM; Schuchman et al., 1991) plays a role in the endocytic process that mediates plasma membrane repair (Idone et al., 2008b).

Results

Blocking lysosomal exocytosis inhibits endocytosis and plasma membrane resealing

Lysosomal exocytosis is partially reduced in cells deficient in factors regulating exocytosis such as synaptotagmin VII and the v-SNARE VAMP7 (Chakrabarti et al., 2003; Rao et al., 2004), whereas complete inhibition is achieved by removing Ca^{2+} from the extracellular medium (Rodríguez et al., 1997). Because plasma membrane repair is also strongly dependent on extracellular Ca^{2+}, we searched for a method to block lysosomal exocytosis without interfering with Ca^{2+} influx. We found that bromoenol lactone (BEL; Fensome-Green et al., 2007) strongly inhibited the extracellular accumulation of lysosomal β-hexosaminidase when cells were wounded by exposure to the bacterial pore-forming toxin streptolysin O (SLO; Fig. 1 A). To determine the effect of BEL treatment on endocytosis, we quantified by EM the number of intracellular vesicles containing the fluid phase tracer BSA-gold 4 min after SLO injury. The number of newly formed endosomes was reduced ∼10-fold in BEL-treated cells (Fig. 1 B), and inhibition was also seen with a quantitative quench-protection endocytosis assay. In this assay, reduction in fluorescence intensity reflects accumulation of WGA-FITC on the plasma membrane because of susceptibility of the WGA-FITC to quenching by membrane-impermeable trypan blue (Fig. 1 C; Idone et al., 2008b). The EM morphology of BEL-treated cells exposed to SLO (swollen ER compartments and less dense cytoplasm) suggested a defect in plasma membrane repair. Flow cytometric detection of the membrane impermeant dye propidium iodide (PI) showed that BEL, while not interfering with the susceptibility of cells to SLO permeabilization or scrape wounding (Fig.1, D and E, Mg^{2+}), abrogated the ability of these cells to reseal efficiently after injury (Fig. 1, D and E, Ca^{2+}). Thus, Ca^{2+}-triggered lysosomal exocytosis seems necessary for the rapid endocytosis previously shown to be involved in plasma membrane repair (Idone et al., 2008b).

Wounded cells secrete the lysosomal enzyme ASM

There is a strong morphological similarity between injury-induced endosomes (Idone et al., 2008b) and the large intracellular vesicles formed in cells treated with bacterial sphingomyelinase (Zha et al., 1998). Because lysosomes contain ASM, an acid-active form of sphingomyelinase, we investigated whether this lysosomal enzyme played a role in the endocytosis-mediated plasma membrane repair process. We found that ASM activity levels in the culture medium increased markedly when cells were permeabilized with SLO in the presence of Ca^{2+}. Consistent with the Ca^{2+} requirement for lysosomal exocytosis, an increase in secreted ASM activity was not observed when extracellular Ca^{2+} was replaced by Mg^{2+} (Fig. 2). These results show that ASM is released from lysosomes into the extracellular medium
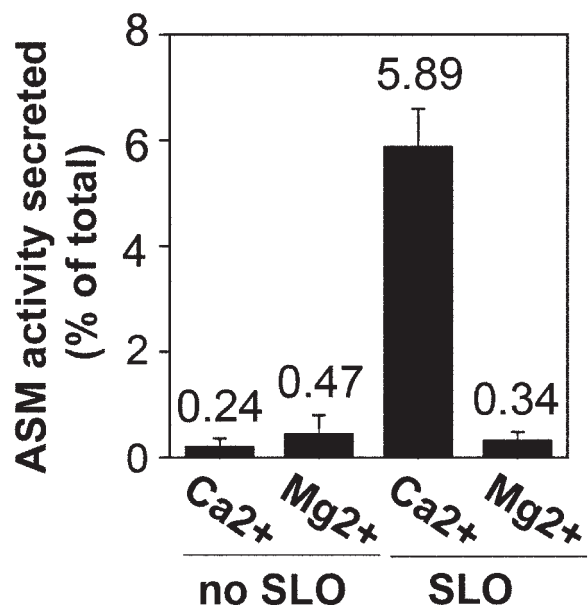

Figure 2. **Cell injury triggers Ca^{2+}-dependent secretion of lysosomal ASM.** ASM activity was assayed in the culture medium of NRK cells 4 min after exposure to SLO. An ∼10-fold increase in secreted ASM activity was observed after exposure to SLO/Ca^{2+}. The data represent the mean ± SD of triplicate determinations. These results are representative of several independent experiments.

during cell injury, gaining access to the outer leaflet of the plasma membrane.

The ASM inhibitor desipramine (DPA) does not impair lysosomal exocytosis but inhibits endocytosis and plasma membrane repair

The exocytosis of active ASM during injury-induced lysosomal exocytosis was consistent with a role for this lysosomal enzyme in the generation of ceramide domains in the plasma membrane, a process which can promote inward budding and vesicle formation (Holopainen et al., 2000; Gulbins and Kolesnick, 2003). To investigate whether ASM activity was required for endocytosis and plasma membrane repair, we first tested the effect of a potent ASM inhibitor, DPA (Kölzer et al., 2004). DPA-treated normal rat kidney (NRK) cells showed a significant reduction (95%) in total ASM activity (Fig. 3 A) but remained capable of vigorous exocytosis of lysosomes upon exposure to SLO in the presence of Ca^{2+} (Fig. 3 B). In contrast, the number of recently formed endosomes in wounded cells was reduced ∼50% by DPA, as determined by EM quantification (Fig. 3 C) and WGA-FITC quench-protection endocytosis assays (Fig. 3 D). DPA treatment inhibited injury-induced endocytosis in cells wounded by either SLO permeabilization or by scraping from the dish (Fig. 3 D). Consistent with the key role of injury-induced endocytosis in plasma membrane repair (Idone et al., 2008a,b), the kinetics of SLO pore removal and plasma membrane resealing were delayed in DPA-treated cells. DPA treatment markedly increased influx of the lipophilic dye FM1-43 in the presence of Ca^{2+} when compared with nontreated cells. Although FM1-43 staining was mostly restricted to the plasma membrane in nontreated wounded cells, after DPA treatment, the dye was able to enter cells and
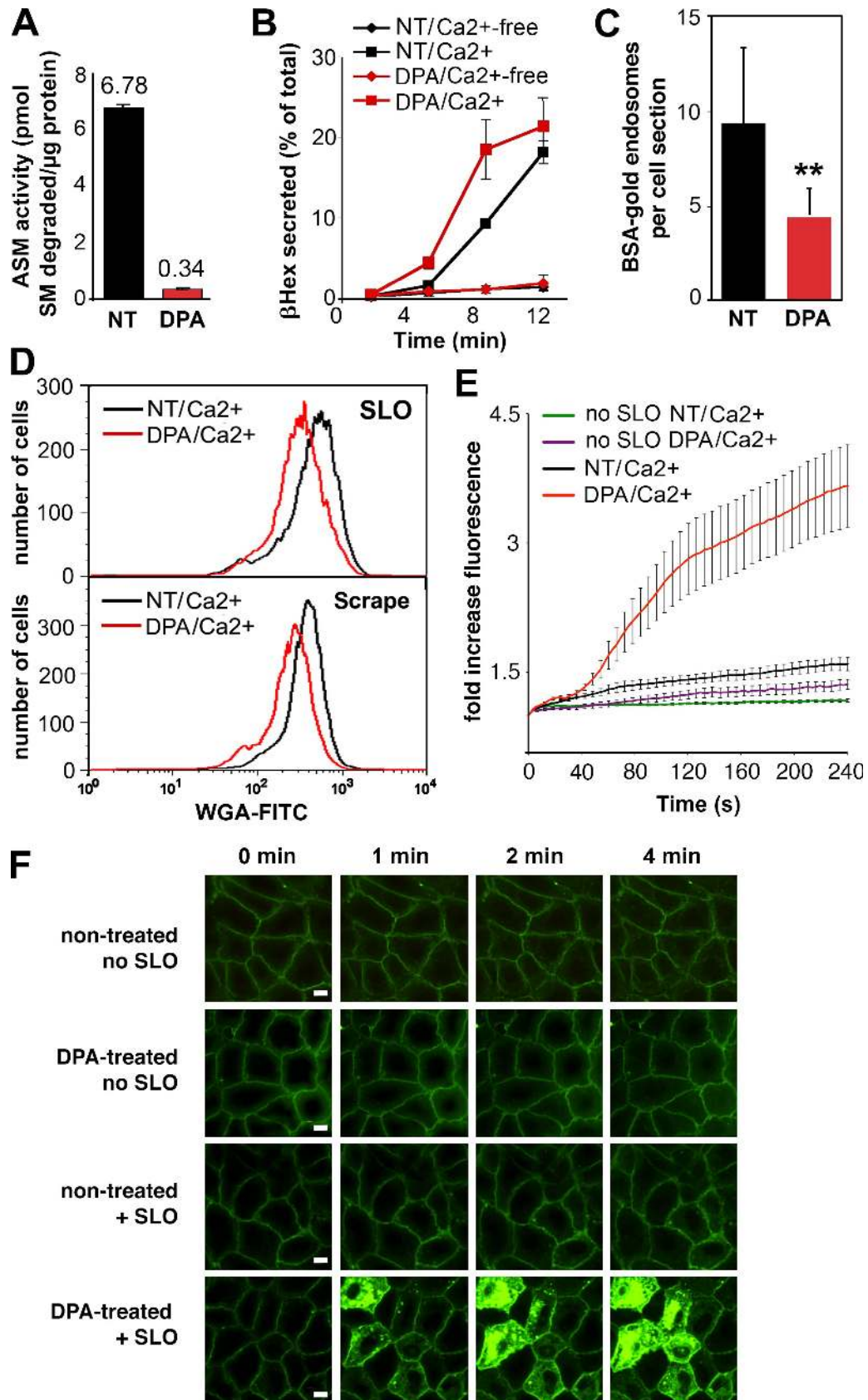
Figure 3. **Blocking ASM activity does not inhibit lysosomal exocytosis but impairs endocytosis and plasma membrane repair.** (A) ASM activity in NRK cell lysates not treated (NT) or treated with DPA (95% inhibition). Error bars represent SEM. SM, sphingomyelin. (B) β-Hexosaminidase (βHex) secretion from nontreated (NT) or DPA-treated NRK cells after exposure to SLO with or without Ca2+. Error bars represent SD. (C) Quantification of BSA-gold–containing endosomes detected by EM in DPA-treated or nontreated cells 4 min after exposure to SLO/Ca^{2+} and BSA-gold. The data represent the mean ± SD

massively stain intracellular compartments (Fig. 3, E and F; and Video 1). FACS analysis of cell populations injured in suspension with SLO and exposed to PI after 4 min also revealed a DPA-dependent defect in plasma membrane resealing (Fig. 4 A). A similar defect was observed in cells injured by scraping (Fig. 4 B). These findings link the lysosomal enzyme ASM to the induction of endocytosis in wounded cells and show that lysosomal exocytosis per se is not sufficient for plasma membrane repair. Despite high levels of lysosomal exocytosis after injury, without active ASM, cells cannot efficiently endocytose and reseal their plasma membrane.

ASM-deficient Niemann-Pick type A (NPA) cells are defective in endocytosis and plasma membrane repair after injury, but resealing is restored by the extracellular addition of recombinant human ASM (rhASM)

We proceeded to directly examine the consequences of ASM deficiency on lysosomal exocytosis, endocytosis, and plasma membrane repair. NPA disease is a lysosomal storage disorder caused by a genetic deficiency in ASM. The lysosomal accumulation of sphingomyelin resulting from deficient ASM activity leads to serious pathology, including aberrant cholesterol metabolism and functional defects in several tissues, particularly the nervous system (Schuchman, 2007). Enzymatic activity assays confirmed that a lymphoblast cell line derived from an NPA human patient contained no detectable ASM when compared with a normal human lymphoblast cell line (Fig. 5 A). The large majority of the control and NPA human lymphoblasts remained impermeable to PI when not exposed to SLO (Fig. 5 B). However, after SLO permeabilization in the presence of Ca^{2+}, a resealing defect that increased with the extent of SLO permeabilization was observed (Fig. 5 C). Both cell types were equally permeabilized, as assessed by the number of cells containing high levels of PI after exposure to SLO under no repair conditions (Fig. 5 C, Mg^{2+}).

These findings were further investigated using fibroblasts from an NPA patient that also lacked detectable ASM activity (Fig. 6 A). When compared with fibroblasts from a normal human patient, NPA fibroblasts showed enhanced β-hexosaminidase secretion after exposure to SLO/Ca^{2+} (Fig. 6 B), similar to what was observed after ASM inhibition with DPA (Fig. 3 B). In contrast, injury-dependent endocytosis (Fig. 6 C) and plasma membrane repair (Fig. 6, D and E; and Fig. 7, A and B) were inhibited in wounded NPA fibroblasts. Control human fibroblasts efficiently resealed their plasma membrane after SLO permeabilization in the presence of Ca^{2+}, effectively blocking the influx of FM1-43 (Fig. 6, D and E; and Video 2) and PI uptake (Fig. 7, A and B). In contrast, NPA fibroblasts were defective in controlling the intracellular flow of FM1-43 (Fig. 6, D and E; and Video 3) and PI after
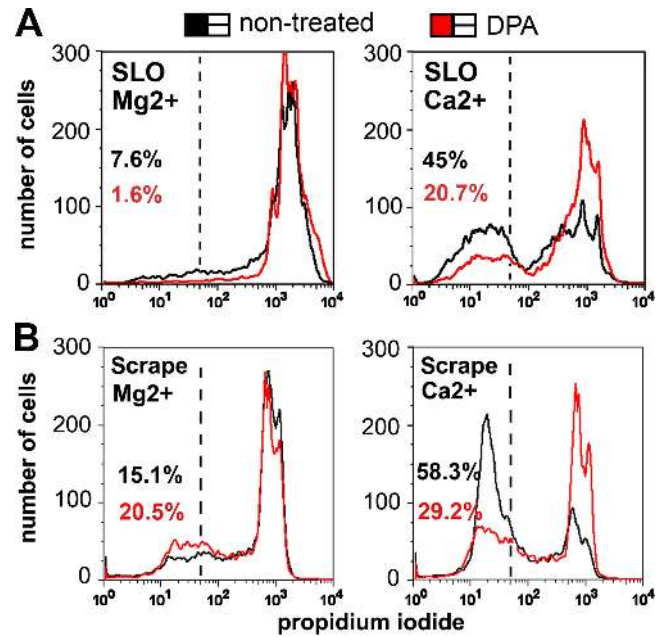

Figure 4. **Inhibition of ASM activity impairs restoration of plasma membrane integrity.** (A) FACS quantification of PI staining in nontreated or DPA-treated cells wounded by SLO permeabilization. (B) FACS quantification of PI staining in nontreated or DPA-treated cells, mechanically wounded by scraping from the dish. Without Ca^{2+} (Mg^{2+}), both groups of cells remained permeabilized; with Ca^{2+}, DPA-treated cells resealed less efficiently than nontreated cells. Percentages correspond to resealed (PI negative) cells in the gated region (dashed lines). The results shown in this figure are representative of several independent experiments.

injury (Fig. 7, A and B). Importantly, when rhASM (He et al., 1999) was added simultaneously with SLO/Ca^{2+}, it restored the ability of NPA cells to reseal their plasma membrane, stopping the influx of FM1-43 (Fig. 6, D and E; and Video 3).

Transcriptional silencing of ASM inhibits endocytosis and plasma membrane repair, a defect reversed by the extracellular addition of rhASM

To determine the consequences of acute ASM depletion, we used siRNA to transcriptionally silence *SMPD1*, the gene encoding for ASM. A reduction of ∼85% in ASM expression, determined with a specific enzymatic assay for ASM activity, was observed in HeLa cells after treatment with an *SMPD1* (ASM) siRNA duplex (Fig. 8 A). Immunoblot analysis confirmed that *SMPD1* (ASM) reduced expression of the ASM protein (Fig. 8 B). When compared with cells treated with control siRNA, EM quantification showed that cells treated with ASM siRNA contained a significantly reduced number of BSA-gold–containing vesicles 4 min after exposure to SLO/Ca^{2+} (Fig. 8 C and Fig. S1). Similar to the endosomes formed after cell injury observed in our previous

(**, P < 0.0001; unpaired Student's *t* test). (D) FACS quantification of WGA-FITC endocytosis in nontreated or DPA-treated NRK cells after SLO exposure or scraping in Ca^2. (E) Time-lapse imaging of FM1-43 influx into NRK cells exposed or not to SLO in the presence of Ca^{2+}. FM1-43 influx was contained in nontreated cells (black) but not in DPA-treated cells (red; Video 1). Cells not exposed to SLO did not show a significant increase in FM1-43 intracellular staining (green and purple). 30–89 cells were analyzed in each condition; error bars correspond to the mean ± SEM. (F) Selected time frames of cells treated or not with DPA but not exposed to SLO and of Video 1 (SLO-exposed cells treated or not with DPA in Ca^{2+}). The results shown in this figure are representative of several independent experiments. Bars, 9 μm.
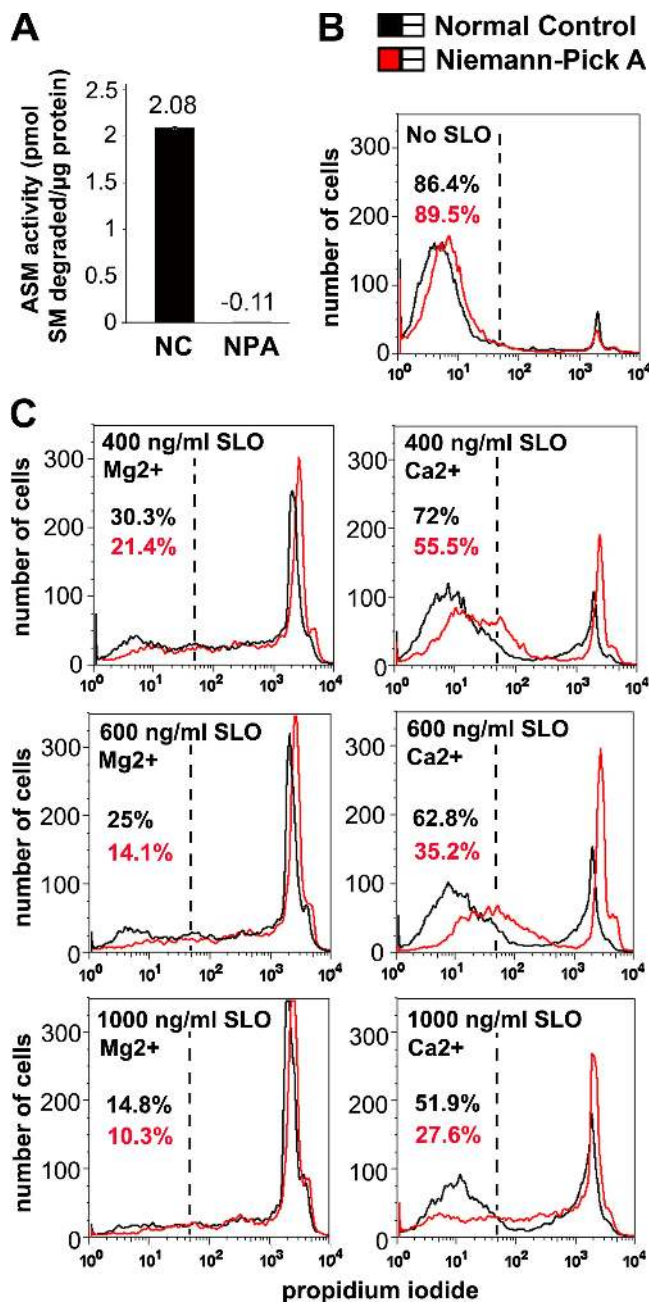
Figure 5. **ASM-deficient NPA lymphoblasts show a defect in plasma membrane repair that is proportional to the extent of cell permeabilization.** (A) ASM activity in lysates of lymphoblasts derived from a normal human control (NC) or an NPA human patient. NPA cells lacked detectable ASM activity. The error bar represents SEM. SM, sphingomyelin. (B) FACS quantification of PI staining in lymphoblasts derived from a normal control or NPA patient. When not exposed to SLO, most cells were impermeable to PI. (C) FACS quantification of PI staining in lymphoblasts derived from a normal control (black) or NPA patient (red) after exposure to SLO. NPA lymphoblasts were defective in plasma membrane resealing when compared with normal lymphoblasts. Without Ca^{2+}, both groups of cells remained permeabilized (left); with Ca^{2+}, control cells resealed more efficiently (right). (B and C) Percentages correspond to resealed (PI negative) cells in the gated region (dashed lines). The results shown in this figure are representative of several independent experiments.

study (Idone et al., 2008b), these vesicles were large and mostly uncoated. Interestingly, in some of these vesicles, areas of localized coat deposition could be detected (Fig. S1 A, top), suggesting

that dynamic sorting events occur in these endosomes after formation. As observed in NPA and DPA-treated cells, plasma membrane repair was also defective in cells subjected to ASM silencing (Fig. 8, D and E; and Fig. S2). Time-lapse imaging assays showed that RNAi-mediated ASM knockdown reduced the efficiency by which cells controlled the influx of FM1-43 after SLO permeabilization in the presence of Ca^{2+} when compared with cells treated with control siRNA (Fig. 8, D and E; and Video 4). As observed with NPA patient cells (Fig. 5 C), FACS-based population assays showed that the defect in plasma membrane repair resulting from siRNA-mediated ASM silencing increased with the extent of cell permeabilization (Fig. S2). The addition of rhASM to the culture medium during SLO permeabilization restored endocytosis (Fig. 8 C) and plasma membrane repair, as indicated by an increased ability of cells to stop the influx of FM1-43 (Fig. 8, D and E) or PI (Fig. S2). Collectively with the rescue of plasma membrane repair in SLO-treated NPA fibroblasts by rhASM (Fig. 6 D and Video 3), these results establish a solid link between extracellular ASM activity and the ability of cells to remove pores from their plasma membrane.

Discussion

In this study, we investigated the relationship between Ca^{2+}-triggered exocytosis of lysosomes and the rapid endocytosis that occurs after plasma membrane injury. Earlier studies established a functional link between lysosomal exocytosis and plasma membrane repair (Reddy et al., 2001; Chakrabarti et al., 2003; McNeil and Steinhardt, 2003), but the precise membrane-resealing mechanism remained elusive. Wound patching by endomembranes delivered to the cell surface by exocytosis was initially thought to be the event responsible for plasma membrane repair (McNeil and Steinhardt, 2003; McNeil et al., 2003). However, a recent study changed this view by showing that plasma membrane lesions can be internalized through a Ca^{2+}-dependent, rapid form of endocytosis (Idone et al., 2008b). By further investigating this pathway, we found that the lysosomal enzyme ASM is released extracellularly during cell injury and participates in the process of endosome formation and plasma membrane repair.

Generation of ceramide on lipid bilayers through the hydrolytic removal of the phosphorylcholine head group of sphingomyelin by sphingomyelinase is known to promote inward bending and budding of membranes (Gulbins and Kolesnick, 2003; van Blitterswijk et al., 2003; Grassmé et al., 2007). The membrane-bending properties of sphingomyelinase-generated ceramide were also directly demonstrated in experiments using liposomes (Holopainen et al., 2000) and implicated in important physiological events such as intraluminal budding in multivesicular endosomes (Trajkovic et al., 2008). Interestingly, in the case of intraluminal budding in multivesicular endosomes, the enzyme implicated was neutral sphingomyelinase 2, which is found in the cytosol (Trajkovic et al., 2008). This is consistent with the opposite topology of luminal budding into multivesicular bodies and endosome formation, which requires exposure of the outer leaflet of the plasma membrane to an extracellular sphingomyelinase. In this study, we provide experimental evidence supporting the
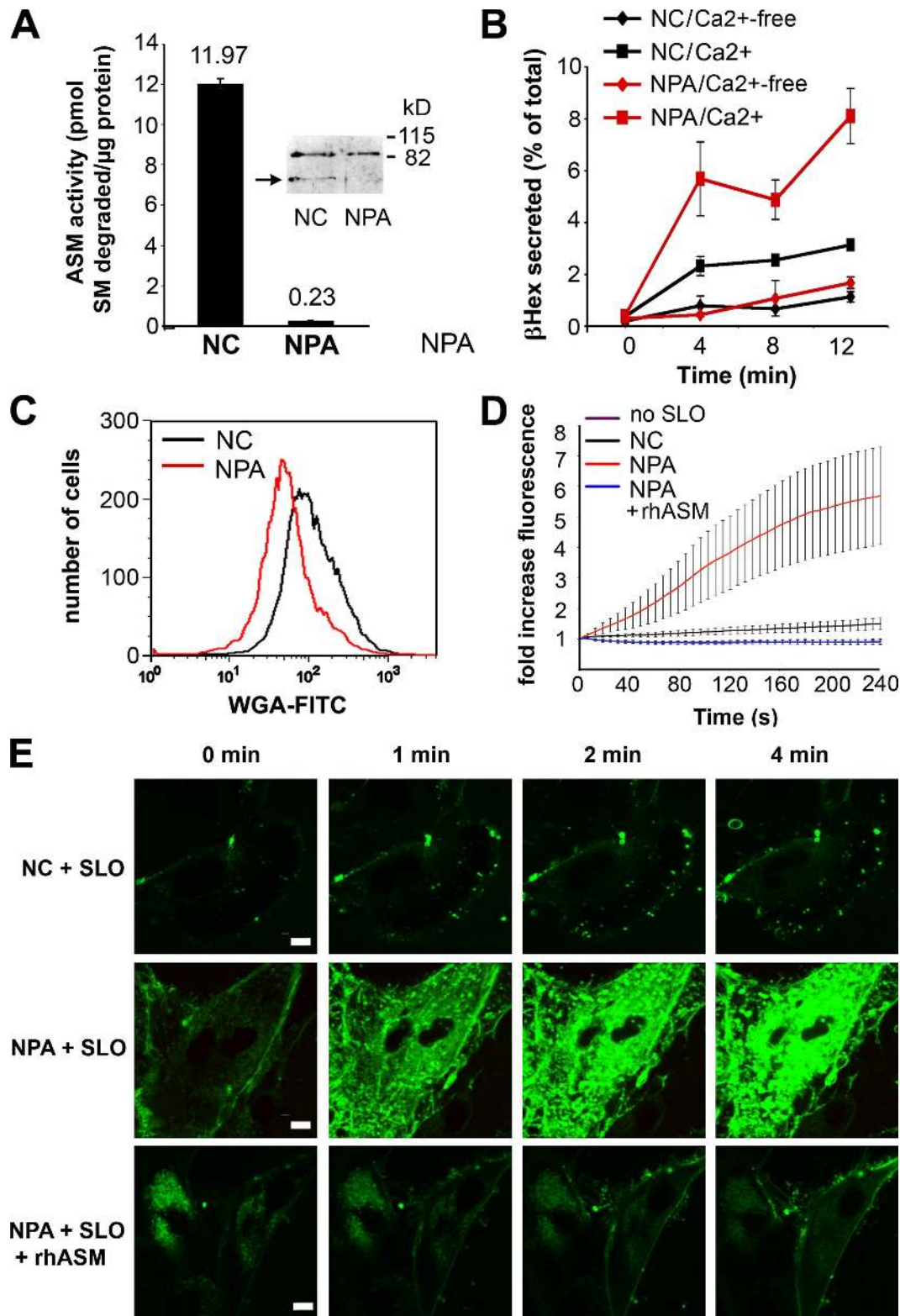
Figure 6. **ASM-deficient NPA fibroblasts are defective in injury-dependent endocytosis and plasma membrane repair.** (A) ASM activity in lysates of normal human fibroblasts (NC) or NPA human fibroblasts. Error bars represent SEM. The inset shows an immunoblot of normal human or NPA fibroblasts using anti-ASM antibodies. The ~75-kD band corresponding to ASM (arrow) was undetectable in NPA cells; the higher additional band is an unspecific reaction. SM, sphingomyelin. (B) β-Hexosaminidase (βHex) secretion from normal human or NPA cells after exposure to SLO with or without Ca^{2+}. Error bars represent SD. (C) FACS quantification of endocytosis after scrape wounding in normal human or NPA cells. (D) Time-lapse imaging of FM1-43 influx into cells exposed or not to SLO in the presence of Ca^{2+}. FM1-43 influx was contained in normal human cells (Video 2) but not in NPA cells. The addition of rhASM at the time of SLO permeabilization restores the capacity of NPA cells to stop FM1-43 influx (Video 3). Non–SLO-permeabilized cells did not show a significant increase in FM1-43 intracellular staining (purple). 4–11 cells were analyzed in each condition; error bars correspond to the mean ± SEM. (E) Selected time frames of Videos 2 and 3. The results shown in this figure are representative of several independent experiments. Bars, 9 μm.
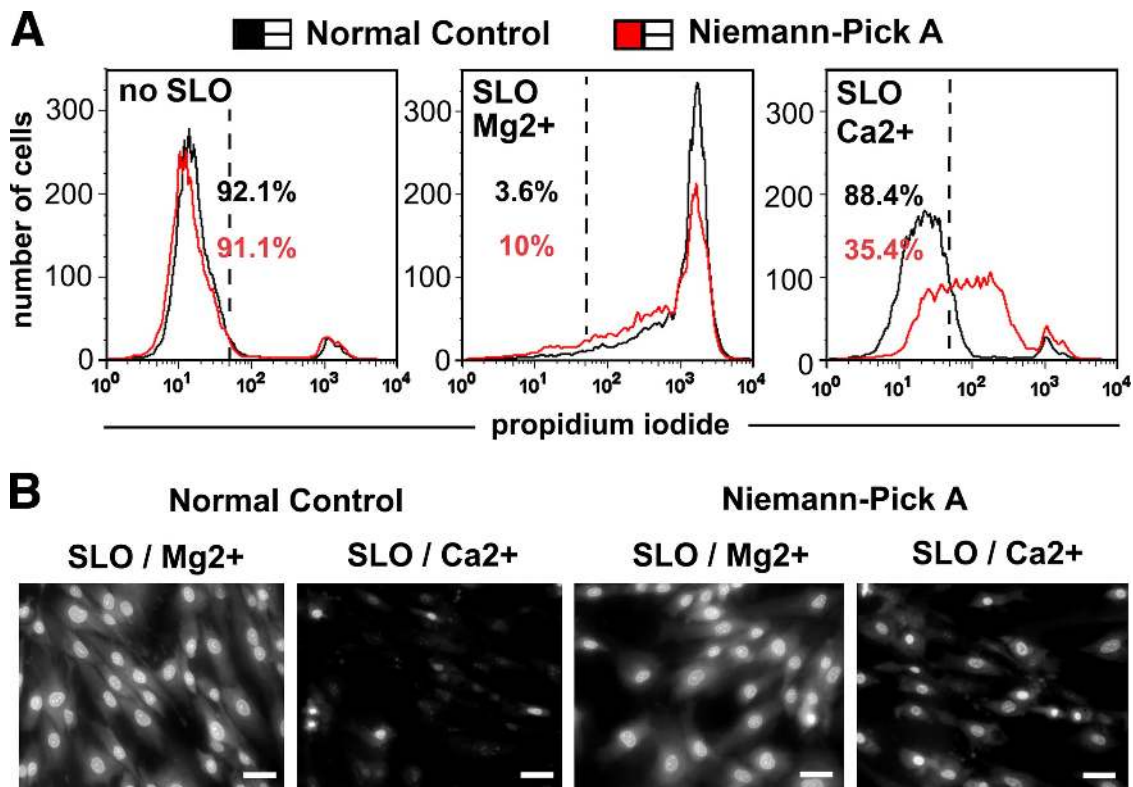
Figure 7. **NPA fibroblasts are deficient in plasma membrane resealing after SLO wounding.** (A) FACS quantification of PI staining in normal control or NPA fibroblasts after SLO permeabilization. Without Ca^{2+} (Mg^{2+}; middle), both groups of cells remained permeabilized; with Ca^{2+}, normal fibroblasts resealed more efficiently (right). Percentages correspond to resealed (PI negative) cells in the gated region (dashed lines). (B) Images of PI-stained normal or NPA fibroblasts permeabilized by SLO. NPA fibroblasts showed increased levels of PI staining after wounding in the presence of Ca^{2+} when compared with normal control fibroblasts. The results shown in this figure are representative of several independent experiments. Bars, 20 µm.

conclusion that ASM, the acidic sphingomyelinase resident in lysosomes, can be exocytosed from injured cells and act on the outer plasma membrane to promote endocytosis.

Our results show that inhibition of ASM release from lysosomes, ASM genetic deficiency, or inhibition/depletion of ASM activity each impair the ability of cells to undergo endocytosis in response to injury and to efficiently reseal their plasma membrane. Furthermore, endocytosis and plasma membrane repair can be restored in ASM-deficient cells by the exogenous addition of the recombinant enzyme. Given that injury-dependent endocytosis and plasma membrane repair occur within a few seconds of membrane wounding (Steinhardt et al., 1994; Idone et al., 2008b), our findings clearly implicate immediate, local effects of ASM-generated ceramide in the outer leaflet of the plasma membrane, as opposed to slower, downstream signaling effects.

Recessive mutations in the ASM-encoding gene (*SMPD1*) are responsible for the human genetic diseases NPA and NPB. NPA patients develop a rapidly progressing neurodegeneration that leads to death in the first 2–3 yr of life. NPB is a milder disease form associated with residual ASM activity (Schuchman, 2007). We found that lymphoblasts and fibroblasts derived from NPA patients have defects in injury-dependent endocytosis and plasma membrane repair that can be rescued by exogenously added ASM. Thus, our observations raise the possibility that defective repair of wounded plasma membrane contributes to the severe pathology that develops in NPA patients. In agreement

with a potential role for ASM in maintaining the integrity of cells subjected to mechanical stress, abnormalities in the permeability barrier properties of skin were reported in a subset of Niemann-Pick patients (Schmuth et al., 2000), and reduced ASM activity levels were detected in patients with atopic dermatitis (Jensen et al., 2004).

One of the main morphological features of NPA cells is the large accumulation of sphingomyelin and cholesterol observed within lysosomes, as a consequence of ASM deficiency. For this reason, the disease was traditionally viewed as a lysosomal storage disorder. However, it has become increasingly evident that another major physiological role of ASM is to initiate ceramide-driven signaling cascades at the cell surface. Extracellular delivery of ASM places this enzyme in direct contact with sphingomyelin, one of the most abundant lipids in the outer layer of the plasma membrane. There is extensive evidence that ASM-mediated hydrolytic removal of the phosphorylcholine head group of sphingomyelin generates extracellularly oriented ceramide platforms on the plasma membrane (Grassmé et al., 2003; Gulbins, 2003; Schuchman, 2010). Several studies detected ASM on the cell surface after exposure to stress signals such as irradiation, heat shock, UV light exposure, or bacterial infection, but the mechanism by which this lysosomal enzyme was released extracellularly has remained obscure (Grassmé et al., 2003; Gulbins, 2003; Schuchman, 2010). Consistent with these observations, cells derived from Niemann-Pick patients or from ASM knockout mice
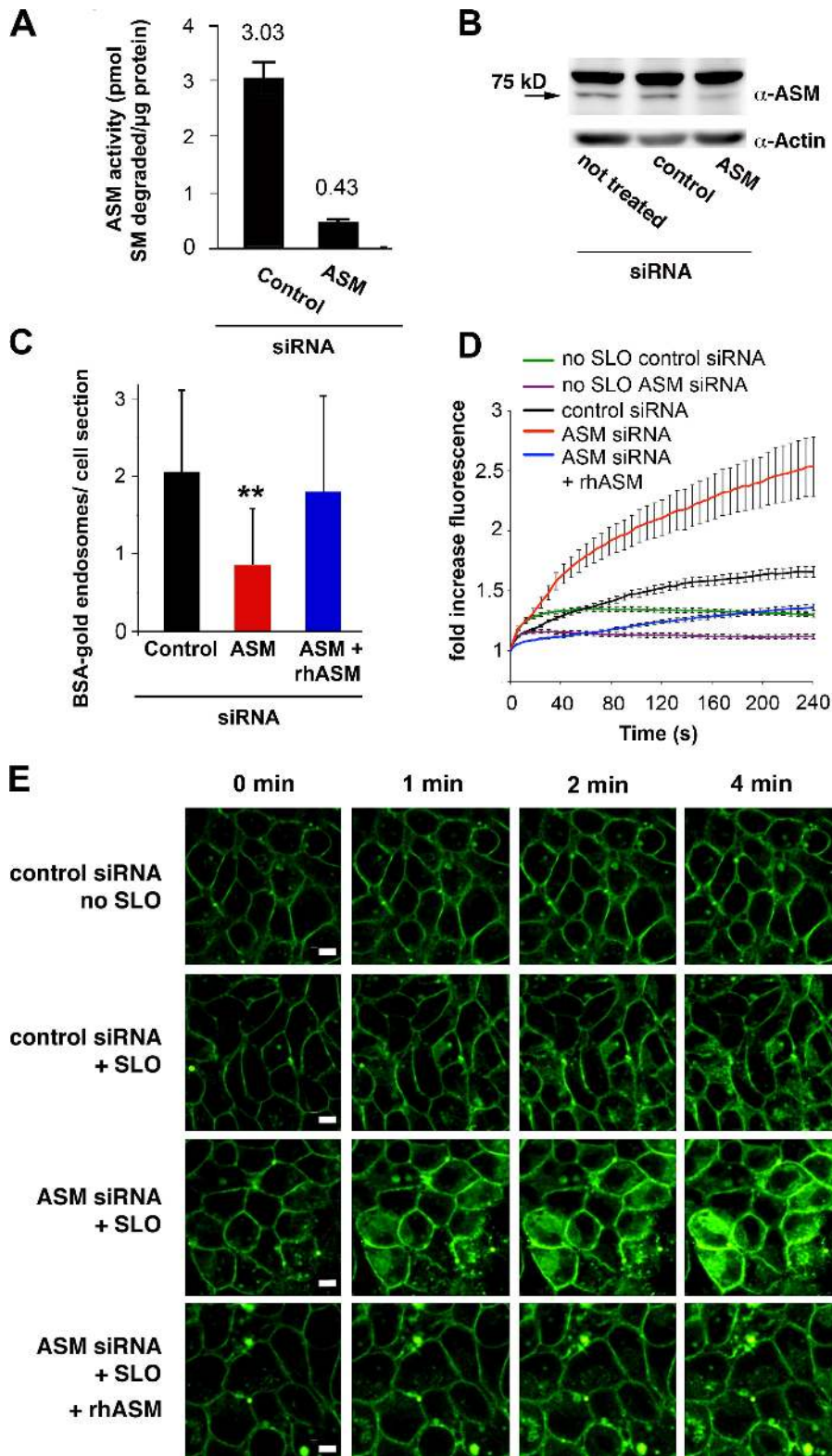
Figure 8. **The defects in endocytosis and plasma membrane repair observed after silencing of ASM expression are rescued by exogenous rhASM.** (A) ASM activity in lysates of HeLa cells treated with control or ASM siRNA. Error bars represent SEM. SM, sphingomyelin. (B) Immunoblots with anti-ASM (top) or antiactin antibodies (bottom) of HeLa cells not treated or treated with control or ASM siRNA. The arrow points to the ~75-kD band corresponding to ASM. The higher additional band is an unspecific reaction. (C) Quantification of BSA-gold–containing endosomes detected by EM in HeLa cells 4 min after exposure to SLO/Ca^{2+} and BSA-gold. The cells were pretreated with control siRNA, ASM siRNA, or ASM siRNA followed by rhASM added during the SLO wounding procedure. The data represent the mean ± SD (**, P < 0.0001; comparing control or ASM + rhASM with ASM by unpaired Student's *t* test). (D) Time-lapse imaging of FM1-43 influx into HeLa cells exposed or not to SLO in the presence of Ca^{2+}. FM1-43 influx was contained in cells treated with control siRNA but not in cells treated with ASM siRNA. The addition of rhASM at the time of SLO permeabilization restored the capacity of NPA cells to stop FM1-43 influx (Video 2). Non–SLO-permeabilized cells did not show a significant increase in FM1-43 intracellular staining (green and purple). 37–63 cells were analyzed in each condition; error bars correspond to the mean ± SEM. (E) Selected time frames of Video 4. Bars, 9 µm.

(which also develop a severe neurodegenerative disease; Horinouchi et al., 1995) are resistant to radiation-induced apoptosis, a defect attributed to disruption of ceramide-mediated signaling cascades normally initiated at the outer leaflet of the plasma membrane (Santana et al., 1996; Schuchman, 2010). Our present results strongly suggest that Ca^{2+} influx through plasma membrane wounds is a major event promoting ASM secretion by triggering the fusion of lysosomal compartments with the plasma membrane. In agreement with this view, we found that ASM activity is not released from cells wounded in the absence of extracellular Ca^{2+}, a condition which does not allow lysosomal exocytosis (Rodríguez et al., 1997; Reddy et al., 2001).
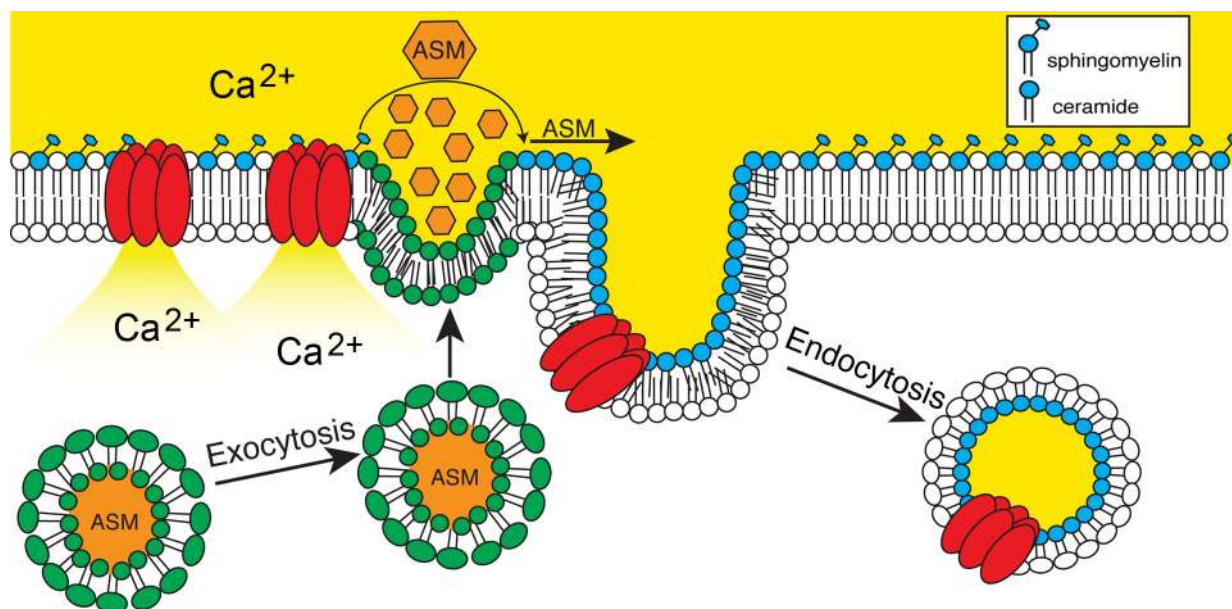
Figure 9. **Model for plasma membrane repair mediated by secreted lysosomal ASM.** Extracellular Ca^{2+} flows into cells through plasma membrane wounds (the diagram shows in red pores formed by insertion of the bacterial toxin SLO). Elevation in the intracellular Ca^{2+} concentration triggers exocytosis of lysosomes. Lysosomal ASM is delivered to the outer leaflet of the plasma membrane, where it converts sphingomyelin into ceramide. Ceramide self-associates into microdomains that bud into the cells, generating endosomes that internalize the lesions and reseal the plasma membrane.

We found that ASM inhibition or genetic deficiency does not impair the exocytosis of the lysosomal enzyme β-hexosaminidase, indicating that lysosomal exocytosis in itself is not sufficient for plasma membrane repair. This finding led us to propose a new model for plasma membrane repair, in which the release of lysosomal contents (as opposed to the delivery of lysosomal membranes) would represent the major event leading to membrane resealing. Our findings are consistent with the following mechanism: Ca^{2+} influx through membrane lesions triggers exocytosis of lysosomes and extracellular release of ASM, which in turn converts sphingomyelin to ceramide in the outer leaflet of the plasma membrane, leading to endosome formation (Holopainen et al., 2000; Gulbins and Kolesnick, 2003) and lesion removal (Fig. 9; Idone et al., 2008b). This model provides for the first time a molecular mechanism by which lysosomal exocytosis can promote endocytosis and plasma membrane repair.

Despite its optimal activity at acidic pH, our reconstitution experiments show that rhASM can act extracellularly, promoting endocytosis and plasma membrane repair under physiological conditions. These findings are consistent with earlier studies showing that ASM has sufficient activity at neutral pH to hydrolyze sphingomyelin within low density lipoprotein particles (Schissel et al., 1998) and to initiate signaling cascades in the outer leaflet of the plasma membrane (Grassmé et al., 2003; Gulbins, 2003). Mechanisms promoting ASM activity in the extracellular environment may include acidic microenvironments generated at the cell surface during lysosomal exocytosis (Baron et al., 1985) or enzyme activation by lysosomal lipids such as lysobisphosphatidic acid (Linke et al., 2001).

Collectively, our results suggest that ASM-dependent endocytosis is a major component of the plasma membrane repair process driven by Ca^{2+} influx. Earlier studies have suggested that Ca^{2+}-dependent cytosolic proteins such as transglutaminase-1

(Inada et al., 2000), calpain (Godell et al., 1997; Mellgren et al., 2007), and mitsugumin 53 (Weisleder et al., 2009) also play a role in cell resealing. However, inhibition of lysosomal exocytosis by a variety of approaches can prevent resealing in the majority of wounded cell populations (Fig. 1; Reddy et al., 2001), indicating that exocytosis of this organelle plays a central role in plasma membrane repair. Interestingly, there is evidence that extracellularly released lysosomal enzymes can activate cytosolic proteins involved in wound repair (Egberts et al., 2004). Future studies should clarify whether additional lysosomal hydrolases delivered to the cell surface by exocytosis participate in the activation of ASM and/or other steps of the pathway leading to restoration of plasma membrane integrity.

Materials and methods

Cells
NRK and HeLa CCL-2.1 (HeLa 229) cells were cultured at 37°C in 5% CO_2 in high glucose DME 10% heat-inactivated FBS containing penicillin/streptomycin (Invitrogen). Normal human fibroblasts (#CRL2522; American Type Culture Collection) and NPA fibroblasts (#GM00112; Coriell) were cultured in DME 20% noninactivated FBS supplemented with 1× MEM nonessential amino acids and 1× vitamin solution containing penicillin/streptomycin (Invitrogen). The human lymphoblast lines MS609AT (normal human patient) and MS2059CK (NPA patient) were from the Schuchman Laboratory and grown in RPMI 1640 10% heat-inactivated FBS containing penicillin/streptomycin (Invitrogen).

Drug treatments
Cells were treated with 50 µM BEL (Sigma-Aldrich) for 30 min or with 30 µM DPA (Sigma-Aldrich) for 60 min before experiments.

ASM transcriptional silencing and complementation with rhASM
HeLa cells (50% confluency) in 35-mm wells containing 250 µl Opti-MEM I reduced serum were transfected with Lipofectamine and 160 pmol of medium GC content control (12935300) or SMPD1 (HSS143988, [RNA]5′-GCCCUGCCGUCUGGCUACUCUUUGU-3′) Stealth siRNA duplexes, according to manufacturer's instructions (Invitrogen). At 55 h after

transfection, cells were exposed to FM1-43 and SLO for imaging assays or trypsinized, washed three times with Ca^{2+}-free DME containing 10 mM EGTA, and exposed to SLO for endocytosis and flow cytometry plasma membrane wounding and repair assays. rhASM with a specific activity of 1 µmol/µg/h at pH 5.0 or 20 nmol/µg/h at pH 7.0, purified to homogeneity in the presence of zinc as previously described (He et al., 1999), was added at 10 µg/ml to the Ca^{2+}-containing DME during the SLO wounding and repair procedures.

Plasma membrane repair assays

Histidine-tagged SLO (carrying a cysteine deletion that eliminates the need for thiol activation) was provided by R. Tweeten (University of Oklahoma, Norman, OK) and purified as described previously (Idone et al., 2008b). Cell monolayers (60% confluence) were washed at 4°C with Ca^{2+}-free DME (containing Mg^{2+} and 10 mM EGTA), followed by two more washes in Ca^{2+}-free DME. SLO was bound to target cells in Ca^{2+}-free DME for 5 min at 4°C, and pore formation was triggered by replacing the medium with 37°C DME containing or not 1.8 mM Ca^{2+}. In all experiments, a titration of SLO was performed to determine the minimum concentration required to permeabilize the whole cell population (150–600 ng/ml, depending on the SLO preparation and target cell type) and the maximum concentration that did not cause cell loss. After 3 min at 37°C, cells were stained for 1 min with 50 µg/ml PI (Sigma-Aldrich) and analyzed by FACS or fixed in 4% PFA and imaged in a microscope (Axiovert 200; Carl Zeiss, Inc.) equipped with a 60× NA 1.25 objective and a camera (CoolSNAP HQ; Photometrics) and MetaMorph software (MDS Analytical Technologies). For FACS assays, 2–4 × 10⁶ trypsinized cells were incubated with SLO in suspension for 5 min at 4°C in 250 µl Ca^{2+}-free DME, followed by resuspension in 37°C DME containing or not Ca^{2+} and PI staining (4-min total incubation time). In scrape wounding assays, cells were removed from the dish at 37°C with a rubber policeman (BD), and PI was added either during scraping or after 4 min at 37°C (5-min total incubation with PI) in the presence or absence of Ca^{2+}. After flow cytometry (FACSCalibur; BD) of at least 10,000 cells, the data were analyzed using FlowJo version 6.3 software (Tree Star, Inc.).

Live time-lapse imaging of FM1-43 influx

Subconfluent cells plated on glass-bottom dishes (MatTek) were preincubated with SLO for 5 min at 4°C, transferred to a LiveCell System chamber (Pathology Devices) at 37°C with 5% CO_2, and exposed to prewarmed DME containing or not Ca^{2+} and 4 µM FM1-43 (Invitrogen) and SLO (Idone et al., 2008b). Spinning disk confocal images were acquired for 4 min at 1 frame/3 s using the UltraVIEW VoX system (PerkinElmer) attached to an inverted microscope (Eclipse Ti; Nikon) with a 40× NA 1.3 objective (Nikon) and equipped with a camera (C9100-50; Hamamatsu Photonics). Quantitative analysis of intracellular fluorescence was performed using Volocity Suite (PerkinElmer).

Exocytosis and endocytosis assays

β-Hexosaminidase secretion assays, which reflect extracellular accumulation of the enzyme resulting from sustained lysosomal exocytosis, were performed as previously described (Rodríguez et al., 1997). Endocytosis was quantified by FACS after SLO or scrape wounding using a trypan blue quenching assay (Loike and Silverstein, 1983; Pearson et al., 2003), as previously described (Idone et al., 2008b). Cells were stained on the plasma membrane with 1 µg/ml WGA-FITC for 1 min on ice, washed three times in PBS, wounded by scraping or by incubation with SLO, and then incubated for 2 min at 37°C. 0.2% trypan blue was then added externally to quench the WGA-FITC fluorescence that remained on the plasma membrane. Because trypan blue does not cross membranes, the WGA-FITC endocytosed during the 2-min incubation at 37°C after wounding was protected from quenching. Cells were then immediately analyzed by FACS for quantifying the reduction in endocytosis after the various treatments (detected as a shift to the left in the fluorescence intensity of the cell population).

For EM endocytosis assays, cells were pretreated with SLO for 5 min at 4°C, incubated for 4 min at 37°C in Ca^{2+}/DME containing BSA-gold (OD 520 nm = 200; Slot and Geuze, 1985) and processed for transmission EM as previously described (Rodríguez et al., 1997). Quantification was performed by counting all vesicles containing BSA-gold (including clathrin-coated vesicles, which corresponded to <7% of all vesicles found in SLO-permeabilized cells after 4 min) in 20–40 cell sections per sample.

ASM detection assays

Cell extracts were prepared by scraping cells into ice-cold 250 mM sucrose followed by 10 passages through a 28-gauge needle. After solvent evaporation, 0.1 µCi of the substrate choline-methyl-[¹⁴C]sphingomyelin

(52 mCi/mmol; PerkinElmer) was resuspended in 20 µl of 100 mM sodium acetate, pH 5.0, and 100 µM $ZnCl_2$ containing 2.7% Triton X-100 and vortexed. The assay solution consisted of 50 µl of assay buffer, 20 µl of substrate, and 20 µl of cell extract. After incubation for 60 min at 37°C, the reaction was terminated by adding 125 µl chloroform/methanol (2:1, vol/vol). Tubes were vortexed and centrifuged at 5,000 g for 5 min at 4°C, and 50 µl of the upper aqueous phase was removed for determination of the amount of [¹⁴C]phosphorylcholine released from [¹⁴C]sphingomyelin by scintillation counting. Samples were normalized for protein concentration using a BCA Protein assay kit (Thermo Fisher Scientific). The ASM activity secreted during cell wounding was measured in a similar manner, except that conditioned medium (from the supernatant of cells after 4 min of SLO treatment at 37°C) was collected and concentrated using Amicon Centriprep YM-10 (Millipore). Secreted ASM activity was expressed as a percentage of the total activity present in cell lysates. Western blotting for ASM was performed on cell lysates separated by SDS-PAGE, transferred to nitrocellulose, and incubated with affinity-purified anti-ASM rabbit antibodies (provided by R. Jenkins and Y. Hannun, Medical University of South Carolina, Charleston, SC) prepared as described previously (Zeidan and Hannun, 2007).

Online supplemental material

Fig. S1 shows that large BSA-gold–positive endosomes are detected in HeLa cells transfected with different siRNA duplex oligonucleotides and injured with SLO. Fig. S2 shows that transcriptional silencing of ASM causes a defect in plasma membrane repair that is proportional to the extent of cell permeabilization and is reversed by the addition of rhASM. Video 1 shows that inhibition of ASM activity with DPA allows rapid and sustained FM1-43 influx into SLO-permeabilized NRK cells. Video 2 shows that normal human fibroblasts control FM1-43 influx after SLO permeabilization. Video 3 shows that NPA fibroblasts are deficient in controlling FM1-43 influx after SLO permeabilization but that the addition of rhASM restores their ability to reseal their plasma membrane. Video 4 shows that HeLa cells treated with ASM siRNA are deficient in controlling FM1-43 influx after SLO permeabilization, a defect which is rescued with the exogenous addition of rhASM. Online supplemental material is available at http://www.jcb.org/cgi/content/full/jcb.201003053/DC1.

References

Baron, R., L. Neff, D. Louvard, and P.J. Courtoy. 1985. Cell-mediated extracellular acidification and bone resorption: evidence for a low pH in resorbing lacunae and localization of a 100-kD lysosomal membrane protein at the osteoclast ruffled border. J. Cell Biol. 101:2210–2222. doi:10.1083/jcb.101.6.2210

Bi, G.Q., J.M. Alderton, and R.A. Steinhardt. 1995. Calcium-regulated exocytosis is required for cell membrane resealing. J. Cell Biol. 131:1747–1758. doi:10.1083/jcb.131.6.1747

Chakrabarti, S., K.S. Kobayashi, R.A. Flavell, C.B. Marks, K. Miyake, D.R. Liston, K.T. Fowler, F.S. Gorelick, and N.W. Andrews. 2003. Impaired membrane resealing and autoimmune myositis in synaptotagmin VII–deficient mice. J. Cell Biol. 162:543–549. doi:10.1083/jcb.200305131

Chambers, R., and E.L. Chambers. 1961. Explorations into the Nature of the Living Cell. Harvard University Press, Cambridge, MA. 352 pp.

Egberts, F., M. Heinrich, J.M. Jensen, S. Winoto-Morbach, S. Pfeiffer, M. Wickel, M. Schunck, J. Steude, P. Saftig, E. Proksch, and S. Schütze. 2004. Cathepsin D is involved in the regulation of transglutaminase 1 and epidermal differentiation. J. Cell Sci. 117:2295–2307. doi:10.1242/jcs.01075

Fensome-Green, A., N. Stannard, M. Li, S. Bolsover, and S. Cockcroft. 2007. Bromoenol lactone, an inhibitor of Group V1A calcium-independent phospholipase A2 inhibits antigen-stimulated mast cell exocytosis without blocking Ca2+ influx. Cell Calcium. 41:145–153. doi:10.1016/j.ceca.2006.06.002

Godell, C.M., M.E. Smyers, C.S. Eddleman, M.L. Ballinger, H.M. Fishman, and G.D. Bittner. 1997. Calpain activity promotes the sealing of severed giant axons. Proc. Natl. Acad. Sci. USA. 94:4751–4756. doi:10.1073/pnas.94.9.4751

Grassmé, H., V. Jendrossek, A. Riehle, G. von Kürthy, J. Berger, H. Schwarz, M. Weller, R. Kolesnick, and E. Gulbins. 2003. Host defense against *Pseudomonas aeruginosa* requires ceramide-rich membrane rafts. *Nat. Med.* 9:322–330. doi:10.1038/nm823

Grassmé, H., J. Riethmüller, and E. Gulbins. 2007. Biological aspects of ceramide-enriched membrane domains. *Prog. Lipid Res.* 46:161–170. doi:10.1016/j.plipres.2007.03.002

Gulbins, E. 2003. Regulation of death receptor signaling and apoptosis by ceramide. *Pharmacol. Res.* 47:393–399. doi:10.1016/S1043-6618(03)00052-5

Gulbins, E., and R. Kolesnick. 2003. Raft ceramide in molecular medicine. *Oncogene.* 22:7070–7077. doi:10.1038/sj.onc.1207146

He, X., S.R. Miranda, X. Xiong, A. Dagan, S. Gatt, and E.H. Schuchman. 1999. Characterization of human acid sphingomyelinase purified from the media of overexpressing Chinese hamster ovary cells. *Biochim. Biophys. Acta.* 1432:251–264.

Heilbrunn, L.V. 1956. The Dynamics of Living Protoplasm. Academic Press, New York. 327 pp.

Holopainen, J.M., M.I. Angelova, and P.K. Kinnunen. 2000. Vectorial budding of vesicles by asymmetrical enzymatic formation of ceramide in giant liposomes. *Biophys. J.* 78:830–838. doi:10.1016/S0006-3495(00)76640-9

Horinouchi, K., S. Erlich, D.P. Perl, K. Ferlinz, C.L. Bisgaier, K. Sandhoff, R.J. Desnick, C.L. Stewart, and E.H. Schuchman. 1995. Acid sphingomyelinase deficient mice: a model of types A and B Niemann-Pick disease. *Nat. Genet.* 10:288–293. doi:10.1038/ng0795-288

Idone, V., C. Tam, and N.W. Andrews. 2008a. Two-way traffic on the road to plasma membrane repair. *Trends Cell Biol.* 18:552–559. doi:10.1016/j.tcb.2008.09.001

Idone, V., C. Tam, J.W. Goss, D. Toomre, M. Pypaert, and N.W. Andrews. 2008b. Repair of injured plasma membrane by rapid Ca²⁺-dependent endocytosis. *J. Cell Biol.* 180:905–914. doi:10.1083/jcb.200708010

Inada, R., M. Matsuki, K. Yamada, Y. Morishima, S.C. Shen, N. Kuramoto, H. Yasuno, K. Takahashi, Y. Miyachi, and K. Yamanishi. 2000. Facilitated wound healing by activation of the Transglutaminase 1 gene. *Am. J. Pathol.* 157:1875–1882.

Jaiswal, J.K., N.W. Andrews, and S.M. Simon. 2002. Membrane proximal lysosomes are the major vesicles responsible for calcium-dependent exocytosis in nonsecretory cells. *J. Cell Biol.* 159:625–635. doi:10.1083/jcb.200208154

Jensen, J.M., R. Fölster-Holst, A. Baranowsky, M. Schunck, S. Winoto-Morbach, C. Neumann, S. Schütze, and E. Proksch. 2004. Impaired sphingomyelinase activity and epidermal differentiation in atopic dermatitis. *J. Invest. Dermatol.* 122:1423–1431. doi:10.1111/j.0022-202X.2004.22621.x

Kölzer, M., N. Werth, and K. Sandhoff. 2004. Interactions of acid sphingomyelinase and lipid bilayers in the presence of the tricyclic antidepressant desipramine. *FEBS Lett.* 559:96–98. doi:10.1016/S0014-5793(04)00033-X

Linke, T., G. Wilkening, S. Lansmann, H. Moczall, O. Bartelsen, J. Weisgerber, and K. Sandhoff. 2001. Stimulation of acid sphingomyelinase activity by lysosomal lipids and sphingolipid activator proteins. *Biol. Chem.* 382:283–290. doi:10.1515/BC.2001.035

Loike, J.D., and S.C. Silverstein. 1983. A fluorescence quenching technique using trypan blue to differentiate between attached and ingested glutaraldehyde-fixed red blood cells in phagocytosing murine macrophages. *J. Immunol. Methods.* 57:373–379. doi:10.1016/0022-1759(83)90097-2

McNeil, P.L., and R.A. Steinhardt. 2003. Plasma membrane disruption: repair, prevention, adaptation. *Annu. Rev. Cell Dev. Biol.* 19:697–731. doi:10.1146/annurev.cellbio.19.111301.140101

McNeil, P.L., S.S. Vogel, K. Miyake, and M. Terasaki. 2000. Patching plasma membrane disruptions with cytoplasmic membrane. *J. Cell Sci.* 113:1891–1902.

McNeil, P.L., K. Miyake, and S.S. Vogel. 2003. The endomembrane requirement for cell surface repair. *Proc. Natl. Acad. Sci. USA.* 100:4592–4597. doi:10.1073/pnas.0736739100

Mellgren, R.L., W. Zhang, K. Miyake, and P.L. McNeil. 2007. Calpain is required for the rapid, calcium-dependent repair of wounded plasma membrane. *J. Biol. Chem.* 282:2567–2575. doi:10.1074/jbc.M604560200

Miyake, K., and P.L. McNeil. 1995. Vesicle accumulation and exocytosis at sites of plasma membrane disruption. *J. Cell Biol.* 131:1737–1745. doi:10.1083/jcb.131.6.1737

Pearson, A.M., K. Baksa, M. Rämet, M. Protas, M. McKee, D. Brown, and R.A. Ezekowitz. 2003. Identification of cytoskeletal regulatory proteins required for efficient phagocytosis in *Drosophila*. *Microbes Infect.* 5:815–824. doi:10.1016/S1286-4579(03)00157-6

Rao, S.K., C. Huynh, V. Proux-Gillardeaux, T. Galli, and N.W. Andrews. 2004. Identification of SNAREs involved in synaptotagmin VII-regulated lysosomal exocytosis. *J. Biol. Chem.* 279:20471–20479. doi:10.1074/jbc.M400798200

Reddy, A., E.V. Caler, and N.W. Andrews. 2001. Plasma membrane repair is mediated by Ca(2+)-regulated exocytosis of lysosomes. *Cell.* 106:157–169. doi:10.1016/S0092-8674(01)00421-4

Rodríguez, A., P. Webster, J. Ortego, and N.W. Andrews. 1997. Lysosomes behave as Ca²⁺-regulated exocytic vesicles in fibroblasts and epithelial cells. *J. Cell Biol.* 137:93–104. doi:10.1083/jcb.137.1.93

Santana, P., L.A. Peña, A. Haimovitz-Friedman, S. Martin, D. Green, M. McLoughlin, C. Cordon-Cardo, E.H. Schuchman, Z. Fuks, and R. Kolesnick. 1996. Acid sphingomyelinase-deficient human lymphoblasts and mice are defective in radiation-induced apoptosis. *Cell.* 86:189–199. doi:10.1016/S0092-8674(00)80091-4

Schissel, S.L., X. Jiang, J. Tweedie-Hardman, T. Jeong, E.H. Camejo, J. Najib, J.H. Rapp, K.J. Williams, and I. Tabas. 1998. Secretory sphingomyelinase, a product of the acid sphingomyelinase gene, can hydrolyze atherogenic lipoproteins at neutral pH. Implications for atherosclerotic lesion development. *J. Biol. Chem.* 273:2738–2746. doi:10.1074/jbc.273.5.2738

Schmuth, M., M.Q. Man, F. Weber, W. Gao, K.R. Feingold, P. Fritsch, P.M. Elias, and W.M. Holleran. 2000. Permeability barrier disorder in Niemann-Pick disease: sphingomyelin-ceramide processing required for normal barrier homeostasis. *J. Invest. Dermatol.* 115:459–466. doi:10.1046/j.1523-1747.2000.00081.x

Schuchman, E.H. 2007. The pathogenesis and treatment of acid sphingomyelinase-deficient Niemann-Pick disease. *J. Inherit. Metab. Dis.* 30:654–663. doi:10.1007/s10545-007-0632-9

Schuchman, E.H. 2010. Acid sphingomyelinase, cell membranes and human disease: lessons from Niemann-Pick disease. *FEBS Lett.* 584:1895–1900. doi:10.1016/j.febslet.2009.11.083

Schuchman, E.H., M. Suchi, T. Takahashi, K. Sandhoff, and R.J. Desnick. 1991. Human acid sphingomyelinase. Isolation, nucleotide sequence and expression of the full-length and alternatively spliced cDNAs. *J. Biol. Chem.* 266:8531–8539.

Slot, J.W., and H.J. Geuze. 1985. A new method of preparing gold probes for multiple-labeling cytochemistry. *Eur. J. Cell Biol.* 38:87–93.

Steinhardt, R.A., G. Bi, and J.M. Alderton. 1994. Cell membrane resealing by a vesicular mechanism similar to neurotransmitter release. *Science.* 263:390–393. doi:10.1126/science.7904084

Togo, T., J.M. Alderton, G.Q. Bi, and R.A. Steinhardt. 1999. The mechanism of facilitated cell membrane resealing. *J. Cell Sci.* 112:719–731.

Trajkovic, K., C. Hsu, S. Chiantia, L. Rajendran, D. Wenzel, F. Wieland, P. Schwille, B. Brügger, and M. Simons. 2008. Ceramide triggers budding of exosome vesicles into multivesicular endosomes. *Science.* 319:1244–1247. doi:10.1126/science.1153124

van Blitterswijk, W.J., A.H. van der Luit, R.J. Veldman, M. Verheij, and J. Borst. 2003. Ceramide: second messenger or modulator of membrane structure and dynamics? *Biochem. J.* 369:199–211. doi:10.1042/BJ20021528

Walev, I., S.C. Bhakdi, F. Hofmann, N. Djonder, A. Valeva, K. Aktories, and S. Bhakdi. 2001. Delivery of proteins into living cells by reversible membrane permeabilization with streptolysin-O. *Proc. Natl. Acad. Sci. USA.* 98:3185–3190. doi:10.1073/pnas.051429498

Weisleder, N., H. Takeshima, and J. Ma. 2009. Mitsugumin 53 (MG53) facilitates vesicle trafficking in striated muscle to contribute to cell membrane repair. *Commun. Integr. Biol.* 2:225–226.

Zeidan, Y.H., and Y.A. Hannun. 2007. Activation of acid sphingomyelinase by protein kinase Cdelta-mediated phosphorylation. *J. Biol. Chem.* 282:11549–11561. doi:10.1074/jbc.M609424200

Zha, X., L.M. Pierini, P.L. Leopold, P.J. Skiba, I. Tabas, and F.R. Maxfield. 1998. Sphingomyelinase treatment induces ATP-independent endocytosis. *J. Cell Biol.* 140:39–47. doi:10.1083/jcb.140.1.39